# Optimal Scheduling of Heat Pumps for Power Peak Shaving and Customers Thermal Comfort

Jochen L. Cremer, Marco Pau, Ferdinanda Ponci and Antonello Monti
*Institute for Automation of Complex Power Systems, E.ON Energy Research Center - RWTH Aachen University, Mathieustrasse 10, 52074 Aachen, Germany*

Keywords: Demand Side Management, Heat Pump Scheduling, Power Peak Shaving, Load Flexibility, Load Balancing, Mixed Integer Linear Programming.

Abstract: Final customers are expected to play an active role in the Smart Grid scenario by offering their flexibility to allow a more efficient and reliable operation of the electric grid. Among the household appliances, heat pumps used for space heating are commonly recognized as flexible loads that can be suitably handled to gain benefit in the Smart Grid context. This paper proposes an optimization algorithm, based on a Mixed-Integer Linear Programming approach, designed to achieve power peak shaving in the distribution grid while providing at the same time the required thermal comfort to the end-users. The developed model allows considering a continuous operation mode of the heat pumps and different comfort requirements defined by the users over the day. Performed simulations prove the proper operation of the proposed algorithm and the technical benefits potentially achievable through the devised management of the heating devices.

## 1 INTRODUCTION

With the evolution towards the Smart Grid (SG) paradigm, new technologies and applications will be put in place to obtain a more efficient, reliable and sustainable utilization of the electric system assets. Some of the most important changes concern the distribution grid, where the penetration of Distributed Generation (DG) and other Distributed Energy Resources (DERs) requires novel management tools to deal with the increasing complexity of the network (Fan and Borlase, 2009). Differently from the past, end-users are also expected to play an active role in the SG scenario. Many customers already evolved into the so-called *prosumers*, thanks to the installation of photovoltaic panels or small wind turbines in their household premises. From one side, this goes in the direction of a more environmentally friendly system, on the other hand it also enables a better use of the network infrastructure if these resources are suitably managed.

Customers' role, however, is not only limited to the installation of generation units based on renewable energy sources, but also includes the possibility to support the grid operation by offering flexibility in the power demand. The exploitation of the flexibility available on the customer side has been a hot research topic in the last years. Several Demand Response (DR) and Demand Side Management (DSM) models have been designed to achieve economic benefits or specific technical goals through the control of different appliances (Balijepalli et al., 2011; Caprino et al., 2014; Klaassen et al., 2016a). Even though many challenges still prevent a wide diffusion of DR and DSM (such as the lack of a suitable regulatory framework, or the absence of the metering and communication infrastructure), the benefits deriving from the application of these schemes are well recognized (Strbac, 2008). As a consequence, it is foreseeable that such applications will play a relevant role in future SGs.

Nowadays, DR schemes are already deployed and well established in the U.S. (US DoE, 2006). From a market perspective the existing programs can be divided in two main categories:

- Price-based programs: customers are motivated to change their demand pattern in response to day ahead or real-time price signals. According to this model, utilities or energy aggregators cannot directly act on end-users appliances but they motivate people to change their power consumption habits usually by offering higher prices in peak hours and lower prices during off-peak hours.
- Incentive-based programs: customers provide to utilities or energy aggregators the possibility to di-



Cremer, J., Pau, M., Ponci, F. and Monti, A.
Optimal Scheduling of Heat Pumps for Power Peak Shaving and Customers Thermal Comfort.
DOI: 10.5220/0006305800230034
In *Proceedings of the 6th International Conference on Smart Cities and Green ICT Systems (SMARTGREENS 2017)*, pages 23-34
ISBN: 978-989-758-241-7

rectly control or schedule some of their appliances and are rewarded for this service through specific incentives in the tariff scheme. In this case, thus, the DR program provider can manage the flexible loads allowed by the customer following his own needs, while fulfilling some customer comfort requirements if this is specified in the agreement.

According to (FERC, 2011), DR programs deployed in U.S. unlock a potential power peak reduction larger than 53 GW. More than 80% of this peak reduction comes from incentive-based programs. This solution, despite being more invasive with respect to the price-based alternatives, allows an optimum management of the load flexibility leading to the certain achievement of the desired targets. Given the invasiveness of these schemes, incentive-based DR is usually implemented to control not critical shiftable or interruptible loads, such as heating devices, air conditioners and water heaters. In Europe, DR and DSM programs are still at an early stage. This is mainly because of the heterogeneity of the regulatory framework in the different countries and, sometimes, also within the same country. Nevertheless, these services are recently being proposed more insistently and DR is regarded as *a key tool to achieve the targets of at least 27% for renewable energy and energy savings by 2030* (SEDC, 2014).

This paper proposes an optimization algorithm conceived to exploit the flexibility provided by heating devices, like heat pumps. Electro-thermal devices are in fact becoming more and more used for space heating, also thanks to the support of recent regulations aimed at improving the energy efficiency in the residential sector. Thanks to the relatively slow dynamics of thermal phenomena, electric heat pumps can be operated flexibly, thus offering a great potential for the deployment of DSM and DR schemes designed for their management (Arteconi et al., 2013). The goal of the optimization algorithm here presented is twofold. The main objective is to minimize the power peaks on the grid, but the heat pumps scheduling is performed also in order to guarantee the thermal comfort required by the end-users.

In the following, Section 2 shows how the flexibility given by heat pumps can be used for DSM purposes and points out the differences between the proposed approach and those already available in literature. In Section 3, the designed optimization algorithm is presented and the constraints taken into account in the used model are described. Section 4 presents the application of the proposed optimization algorithm in different case studies, highlighting the technical benefits potentially achievable through the devised heat pumps management. Section 5 finally summarizes the obtained results and concludes the paper.

## 2 USE OF HEAT PUMPS FOR DEMAND SIDE MANAGEMENT

The flexibility provided by heating systems has been studied and evaluated in several works, proving that a large potential exists for the application of DR schemes based on the management of electro-thermal devices (Klaassen et al., 2016b; Chapman et al., 2016). As a consequence, large efforts have been focused on this research field, dealing with different aspects like the modelling of the thermal system (Good et al., 2013; Akmal and Fox, 2016) or the estimation of the heating demand (Kouzelis et al., 2015) in order to design tailored DR schemes. Many of the DSM and DR programs proposed in the literature refer to the price-based model and aim at minimizing the costs incurred by the final customer. Therefore, the developed models are usually conceived as a service to the customer, while the utilities can address their needs (in terms of grid management) by sending different price signals over the time and relying on the response of the users to the varying prices.

In (Molitor et al., 2011), different price schemes are used as input to an optimization algorithm running at the end-user premises for the scheduling of heat pumps. Results show that the optimal scheduling leads to a reduction of the energy consumption of the customer, but this is obtained at the expense of a thermal discomfort. In (Loesch et al., 2014), an evolutionary algorithm is proposed to schedule the heat pump so to minimize the costs for the user, given the price of the energy in the spot market. Here utilities can also define power limitations in specific periods of the day for solving possible contingencies in their grid and charge penalties to the customer if such limitations are not respected. The algorithm is able to exploit the flexibility provided by the heating system and to minimize the user costs, but a direct link to the thermal comfort delivered to the customer is missing. The proposal in (Bhattarai et al., 2014) also tries to combine the objective of minimizing the costs for the customer with a service that is oriented to the distribution grid management. A two-step optimization process is presented, where the first step gives the scheduling of the heat pumps (minimizing the costs) while the second step checks possible voltage problems in the grid and, in case, shifts the heat pumps operation to the following time slots. Again, customer discomfort is in general possible in case of reallocation of the heat pumps operation. Heat pump flexibility is directly used to improve the operation of distribution grids in (Csetvei et al., 2011). A method to define local price signals for the end-users is presented, where additional costs are added to the spot market prices if overload conditions exist. The price signals are then used to determine the set point temperature of the heat pumps. The method allows eliminating the overloads, but customer discomfort can still arise during overload periods.

To avoid thermal discomfort for the end-user, some proposals include in the optimization model constraints on the indoor temperature provided to the customer. In (De Angelis et al., 2013), temperature boundaries are considered in a home energy management system which is used to schedule the operation of flexible loads (including heat pumps) and possible storage systems. The objective is to reduce the costs for the customer, so utilities can pursue their goals only by setting different price signals over the time. In (Nielsen et al., 2012), instead, the price-based scheme is compared to two different DR approaches where the power consumption or the temperature set point of the heat pump are directly controlled by the DR provider. The objective is in this case to minimize the costs for the energy aggregator (which is providing the DR program), while minimizing the discomfort for the customers by keeping their home temperature between the considered boundaries. Similarly to the case of the heat pumps, (Li et al., 2017) propose an algorithm to manage air conditioners by acting on the temperature set points in order both to reduce energy consumption and to provide the interruptibility of the load as DR service. In this case, no fixed temperature boundaries are used, but the control scheme was tested in the field and tuned according to the customers feedback in order to minimize their thermal discomfort.

All these approaches, while proposing solutions to make DR and DSM programs more attractive for the final customer, do not allow to fully exploit the available flexibility for enhancing the efficiency of the electric system operation. As described in (Strbac, 2008) and reported in (US DoE, 2006), one of the main benefits for the system would be the power peak minimization. By minimizing the power peaks in the grid, utilities can minimize power losses, improve the voltage profile in the grid, reduce the risk of contingencies and postpone network reinforcement in areas with increasing connected power. At system level, this also leads to avoid the use of expensive generation units during peak hours and to reduce the needed spinning reserve, thus minimizing the overall costs.

For this reason, differently from the other proposals available in the literature, the DSM model here presented performs an optimal day ahead scheduling

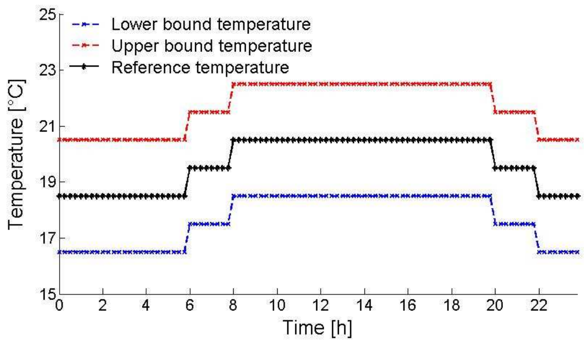


Figure 1: Example of user-defined comfort requirement.

of the heat pumps for minimizing the power peaks on the grid over the day. The minimization is performed by taking into account user-defined requirements in terms of thermal comfort, so that both utilities and end users can take advantage from the proposed DSM program. Further reward to the final customers could be also defined, in terms of incentives in their tariff, to make the DSM scheme more appealing, depending on the savings the utilities estimate to achieve from the application of this optimization on a large scale.

## 3 MODEL FORMULATION

This section presents the formulation used for the proposed DSM model. First, the thermal model, consisting of comfort constraints, boundary constraints, energy balance equations and heat pump equations/constraints, is described. Then, the optimization algorithm designed to perform the day ahead scheduling of the heat pumps in the considered grid is presented.

### 3.1 Thermal Model

**Comfort constraints** They are used in the model to guarantee the comfort requirements of the residents living in each house. In the proposed DSM scheme, users choose the reference temperature they want to have (it can also vary during the day) and provide a certain boundary around such reference temperature. Figure 1 shows an example of possible temperature requirement for a customer. The comfort constraints are thus defined so that, for every time period $t$, the indoor temperature is always within the permitted range. Indicating with $\Gamma^{LB}_{h,t}$ and $\Gamma^{UB}_{h,t}$ the lower and the upper bound, respectively, of the temperature in house $h$ at time $t$, the following holds:

$$T^{IN}_{h,t} \geq \Gamma^{LB}_{h,t} \qquad \forall h,t \qquad (1a)$$

$$T^{IN}_{h,t} \leq \Gamma^{UB}_{h,t} \qquad \forall h,t \qquad (1b)$$

where $T^{IN}_{h,t}$ is the variable associated to the indoor temperature of house $h$ at time $t$.

**Boundary constraints** They are added to define the initial and final states of the temperature for the daily optimization. Given a starting temperature $\Gamma^{INI}_{h}$, the temperature at time $t = 0$ is:

$$T^{IN}_{h,0} = \Gamma^{INI}_{h} \quad \forall h \tag{2}$$

while at the final time period $f$, the indoor temperature is bounded with the inequality constraint:

$$T^{IN}_{h,\mathrm{f}} \geq \Gamma^{REF}_{h,\mathrm{f}} \quad \forall h, \tag{3}$$

where $\Gamma^{REF}_{h,\mathrm{f}} = \frac{\Gamma^{UB}_{h,\mathrm{f}}+\Gamma^{LB}_{h,\mathrm{f}}}{2}$ is the reference temperature of house $h$ at $t = \mathrm{f}$. Such a choice is done in order not to have a final temperature too close to the lower bound, since this would force to turn on the heat pump at the beginning of the following day (thus removing any flexibility for the first time steps of the subsequent day ahead scheduling).

**Energy balance** The energy balance equation defines how the indoor temperature changes over the time due to the heat provided by the heat pump and the heat loss to the outdoor environment. The used equation is based on the model described in (De Angelis et al., 2013) and it is:

$$T^{IN}_{h,t} = T^{IN}_{h,t-1} + \frac{\Delta t}{\mu^{HS}_{h}\,\gamma^{AR}} \left(Q^{HP}_{h,t} - Q^{LS}_{h,t}\right) \quad \forall h,t \tag{4}$$

where $\Delta t$ is the duration of the time period between two consecutive discrete time steps, $\mu^{HS}_{h}$ and $\gamma^{AR}$ are specific parameters, namely the house indoor air mass and the air heat capacity, and $Q^{HP}_{h,t}$ and $Q^{LS}_{h,t}$ are variables indicating the heat flow given by the heat pump and the heat loss, respectively.

The indoor air mass $\mu^{HS}_{h}$ is a parameter that depends on the size and geometrical characteristics of the house (see (De Angelis et al., 2013) for more details) and, combined with the air heat capacity $\gamma^{AR}$, appears as a thermal energy storage for the house, thus affecting the dynamics of the thermal phenomena.

The heat losses are instead defined through the following relationship:

$$Q^{LS}_{h,t} = \kappa^{HS}_{h} \left(T^{IN}_{h,t-1} - \Gamma^{OT}_{h,t-1}\right) \quad \forall h,t \tag{5}$$

Such losses depend on a heat loss factor $\kappa^{HS}_{h}$ and on the temperature difference between the indoor and the outdoor temperature $\Gamma^{OT}_{h,t-1}$.

As for $Q^{HP}_{h,t}$, more details will be provided in the following paragraph where the used heat pump model is fully described.

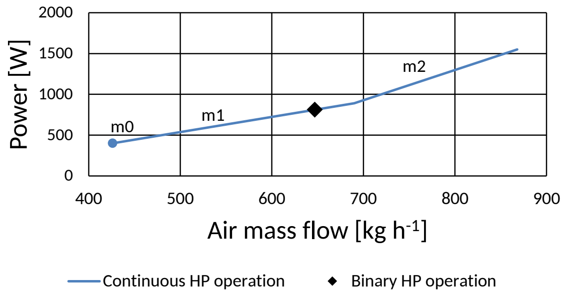


Figure 2: Power demand of the heat pump in binary or continuous mode.

**Heat pump model** This model has to link the delivered heat $Q^{HP}_{h,t}$ to the electrical power $P^{HP}_{h,t}$ required to produce such heat, and has to account for all the possible constraints present in the heat pump operation. In the literature, heat pumps are often considered to work at a fixed power and thus a simple binary variable is adopted to define if their status is on or off. In some papers, a multi-operation mode is instead defined by considering different discrete air mass flows to which different electrical powers are consequently associated. In this case, binary variables are introduced for each discrete operation mode, hence determining an increasing complexity of the optimization problem. In this paper, a continuous operation mode of the heat pump is considered. This means that the heat pump can generate any value of air mass flow included in the range between a minimum and a maximum limit. The electrical power needed to generate the output air mass flow can be described through a function, which can be in first approximation linearised through a given number of linear segments. Figure 2 shows an example of linearised curve mapping the air mass flow to the required electrical power, which has been obtained using heat pump data given in (De Angelis et al., 2013).

In Figure 2, it is possible to observe that three operation modes are defined: the first one, named m0, is a discrete value corresponding to the minimum air mass flow of the heat pump; the second one, m1, is associated to the first segment of the curve; the last one, called m2, is linked to the upper segment of the curve and arrives till the maximum air mass flow for the heat pump. As it will be shown in the following, such a solution can be implemented in the optimization algorithm by using integer variables for each operating mode, while just one binary value is used to determine the status (on or off) of the heat pump. Figure 2 also shows the possible limits present in the definition of a simple binary operation mode for the heat pump. In fact, in such a case a single operating point of the heat pump has to be decided, which does not reflect the actual operation mode of many heat pumps.

Relying on the described continuous operation, the generated heat is defined as:

$$Q_{h,t}^{HP} = \gamma^{AR} \sum_{m} \Delta F_{h,m,t}^{HP} \left(\Gamma_{h}^{HP} - \Gamma_{h,t-1}^{RF}\right) \quad \forall h,t \tag{6}$$

where $\Gamma_{h}^{HP}$ is the output temperature of the heat pump (assumed as constant) and $\Gamma_{h,t-1}^{RF}$ is the reference temperature of the house $h$ at the time step $t-1$. It is worth noting that a rigorous definition of the generated heat $Q_{h,t}^{HP}$ would require the use of the actual indoor temperature $T_{h,t-1}^{IN}$ in (6) in place of the reference temperature $\Gamma_{h,t-1}^{RF}$. However, such a solution would lead to a nonlinear relationship and for this reason it is here approximated by using the constant value given by $\Gamma_{h,t-1}^{RF}$. This approximation is considered acceptable since the indoor temperature is constrained to be close to the reference temperature due to the comfort constraints previously defined.

The other term appearing in (6), namely $\Delta F_{h,m,t}^{HP}$, is the additional air mass flow of mode $m$ with respect to the upper bound air mass flow of mode $m-1$. As for the first operating mode m0, the air mass flow is constrained by the following equality constraint:

$$\Delta F_{h,\mathrm{m0},t}^{HP} = y_{h,t}\ \Phi_{h,\mathrm{m0}} \quad \forall h,t. \tag{7}$$

where $\Phi_{h,\mathrm{m0}}$ is the minimal air mass flow of the heat pump. The air mass flow of mode m0 is thus either 0 or $\Phi_{h,\mathrm{m0}}$ depending on the binary decision variable $y_{h,t}$. The additional air mass flows of all other operating modes $m$ are instead constrained by the following inequality constraints:

$$\Delta F_{h,m,t}^{HP} \leq y_{h,t}\ \Delta\Phi_{h,m}^{UB} \quad \forall h, m \notin \{\mathrm{m0}\}, t \tag{8}$$

where $\Delta\Phi_{h,m}^{UB}$ is the upper bound of the additional air mass flow of the linearised segment associated to mode $m$.

Given these definitions of the additional air mass flows, the required power of the heat pump is directly mapped to the air mass flow by means of the following equation:

$$P_{h,t}^{HP} = \sum_{m} \beta_m \Delta F_{h,m,t}^{HP} \quad \forall h,t \tag{9}$$

where the parameter $\beta_m$ is the power per air mass flow associated to each mode $m$. The total power of the heat pump is thus determined by taking the sum of all the additional air mass flows $\Delta F_{h,m,t}^{HP}$ multiplied by the respective parameter $\beta_m$ over all the operating modes $m$. The proposed formulation works properly for increasing values of $\beta_m$ ($\beta_{\mathrm{m0}} \leq \beta_{\mathrm{m1}} \leq \beta_{\mathrm{m2}} \ldots$) as in Figure 2. In fact, since the following optimization operates to minimize the used powers, this ensures that the modes will be automatically selected by the solver in the order $m = \{\mathrm{m0}, \mathrm{m1}, \mathrm{m2} \ldots\}$.

A further aspect considered in heat pump model is the possible presence of time constraints. These constraints account for the minimum (or maximum) times the equipment has to operate or have to be turned off since, usually, many operational switches result in inefficiency and mechanical stress. In (Hedman et al., 2009), several different methods to account for time constraints in another scheduling problem (the unit commitment problem) were proposed and examined. Results of such work are here adapted to the heat pump scheduling problem. In this case, only a minimum number of time periods $\tau$, during which the heat pump has to be turned on, is implemented (e.g., no minimum turn-off time) by the two following constraints:

$$Z_{h,t} \geq y_{h,t} - y_{h,t-1} \quad \forall h,t \tag{10}$$

$$\begin{aligned} Z_{h,t} \leq & y_{h,\tau} \\ & \forall h,t,\tau \in \{t, \cdots, \min(t+\tau^{MIN}-1, \mathrm{f})\}. \end{aligned} \tag{11}$$

Note, the switching variable $0 \leq Z_{h,t} \leq 1$ is a bounded continuous variable. Therefore by using these time constraints, the introduction of new binary variables is not required. More binary variables would result in a larger branch and bound tree and thus in a more complicated problem. As a result, the complexity of the problem decreases by using the inequality constraints proposed in (10) and (11).

## 3.2 The Optimization Algorithm

As discussed in Section 2, the objective of the DSM here proposed is to minimize the power peaks in the grid. To achieve this target, Quadratic Programming (QP) could be used to minimize the squared power resulting on the monitored network over all the time periods. However, if binary variables are included in the problem, QP approaches lead to very high computational burden and execution times. For this reason, in the proposed approach, the objective function has been linearised as presented in the following. This, together with the linear constraints defined in Section 3.1, allows obtaining a linear problem that can be solved more easily through a Mixed Integer Linear Programming (MILP) formulation. In this way, execution times can be reduced, which is an essential aspect when dealing with large optimization problems (in this scenario, when optimizing the heat pump operation of a large number of houses).

The basic idea used here to linearise the objective function is to discretize the power consumption at time $t$ through a given number of blocks $b$ and to assign increasing weights to blocks associated to higher levels of power (see Figure 3); in this way, the minimization of the weighted blocks leads to avoid

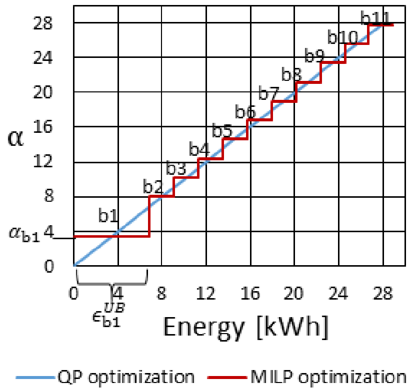


Figure 3: The weight $\alpha_b$ of the energy $\Delta E_{b,t}$ in box $b$.

the allocation of flexible load consumption in periods where power peaks are occurring. These blocks can be interpreted as boxes that can be filled with energy up to their respective capacity $\varepsilon_b^{UB}$. Each energy box $b$ is thus a continuous variable (indicated in the following with $\Delta E_{b,t}$) that is lower bounded by 0 and upper bounded through this inequality constraint:

$$\Delta E_{b,t} \leq \varepsilon_b^{UB} \quad \forall t \tag{12}$$

where $\varepsilon_b^{UB}$ is the maximum capacity of the energy box, which, in general, can be different for each block $b$.

For each time step $t$, the sum of all the energy boxes is related to the power consumption in that period by means of:

$$\sum_b \Delta E_{b,t} \geq \sum_h \Delta t P_{h,t}^{HP} + \varepsilon_t^{GD} \quad \forall t \tag{13}$$

where $\varepsilon_t^{GD}$ is the energy consumption at time $t$ given by all the non-scheduled loads in the grid and $P_{h,t}^{HP}$ is the already mentioned power consumption of the heat pumps for each house $h$.

Given the above definition of the energy boxes and considering all the constraints introduced in the problem, the optimization used to schedule the heat pumps is a centralized algorithm with the following objective function:

$$\begin{aligned} &\underset{y_{h,t},\Delta F_{h,m,t}^{HP}}{\text{minimize}} && \sum_t \sum_b \alpha_b \, \Delta E_{b,t} \\ &\text{s.t.} && \text{Eqs. } (1)-(13). \end{aligned}$$

where the optimization decisions are the binary variables $y_{h,t}$ and the continuous variables $\Delta F_{h,m,t}^{HP}$. As it can be observed, the designed algorithm is thus a centralized approach where the heat pumps of each house included in the problem are scheduled within the same DSM optimization procedure. Similarly to the case of the additional air mass flows, for the

Table 1: Parameters of the heat pump.

| Mode $m$ | m0 | m1 | m2 |
|---|---|---|---|
| $\beta_m^{HP}(\mathrm{W\,h\,kg^{-1}})$ | 0.939 | 1.86 | 3.70 |
| $\Delta\Phi_m^{UB}(\mathrm{kg\,h^{-1}})$ | 426 | 264 | 178 |

proper functioning of the method it is crucial that the weight $\alpha_b$ is increasing ($\alpha_{b1} \leq \alpha_{b2} \leq \alpha_{b3} \ldots$). In this case, indeed, the boxes will be selected (or 'filled with energy') by the solver in the order $b = \{b1, b2, b3 \ldots\}$. The box approach is reasonable since the target is only the cut of the highest peak. This approach allows to be tailored to the considered scenario. For example, the discretization in the energy level can be modified, or any arbitrary strong functions (e.g., exponential to the power $x$, etc.) can be linearized by setting the values of the weights $\alpha_b$ accordingly. Differently from other proposals available in literature and, in general, from price-based DSM schemes, the proposed centralized approach also allows avoiding that possible high power peaks are simply shifted from a time to another due to the similar response of the customers to the DSM inputs.

# 4 TESTS AND RESULTS

## 4.1 Tests Setup

The proposed optimization algorithm has been tested considering different scenarios where the DSM provider wants to minimize the power peak of the grid using the flexibility provided by 60 residential houses endowed with electric heat pumps. The time horizon for the scheduling is one day. The initial time of the scheduling problem is midnight and the day is separated in 96 time periods resulting in a discretization time step of $\Delta t = 15\,\text{min}$. For the sake of simplicity, in the simulation it is assumed that all houses have the same heat pump that can continuously operate in 3 different modes. However, the algorithm obviously allows for the implementation of heat pumps with different characteristics for each house $h$. The parameters of the heat pump model are stated in Table 1 and are derived from (De Angelis et al., 2013). It is worth reminding that mode m0 is the operating start point, while the linear operating segments m1 and m2 offers continuous operation of the heat pump as depicted in Figure 2. The output temperature of the heat pump has been chosen as $\Gamma^{HP} = 30\,°\mathrm{C}$ and the minimal time period the heat pump has to run is $\tau = 2$ (corresponding to a minimal operation time of 30 min).

As shown in Figure 4, in the proposed DSM scheme, the inputs needed for the optimization algorithm are:

- a forecast of the inflexible load in the grid
- a forecast of the outdoor temperature
- the thermal comfort required by the customers, together with heat pumps and building characteristics.

As for the inflexible load profile in the grid, statistical data are often available (for example at substation level) regarding the aggregated power consumption in different periods of the year and for different types of day (e.g. working or weekend day). In the following simulations, the aggregated profiles of residential houses have been taken from the standard load profile of 2012 (Bundesverband der Energie- und Wasserwirtschaft) using an average consumption of 2000 kWh/year per customer. Two different periods of the year, namely a working day in May and one in December, have been simulated, and the corresponding load profiles have been assumed as inflexible load for the residential customers. In addition, the presence of industrial consumers has been also considered. This contributes to give the final shape of the forecast inflexible load, as it will be shown in the next subsection when presenting the simulated scenarios.

For the forecast of the outdoor temperature, the actual temperature of a day in May is used in a first simulation, while the actual temperature of a day in December is used to simulate a second scenario. The used temperature profiles are presented in Figure 5. The thermal comfort of the 60 houses differs from house to house and individual parameter sets (as described in the previous section) have to be taken into account. For the case studies presented here, the relevant parameters are sampled based on 5 different temperature profiles and 12 different building characteristics. Figure 5 shows the 5 different temperature profiles (the reference temperature is always the mean

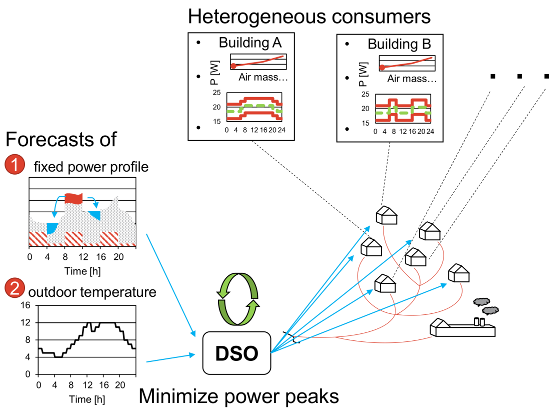


Figure 4: Overall model of the designed DSM scheme.

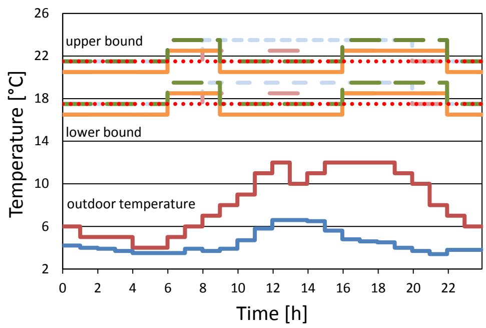


Figure 5: Upper and lower temperature bounds of the residents and outdoor temperature.

value of the upper and lower bound). As starting point for the simulation, the initial indoor temperature $\Gamma_h^{INI}$ is assumed to be equal to the reference temperature of the first time period. The 12 building types differ in the indoor air mass and the heat loss factor (Figure 6). The parameters are calculated based on the geometric dimensions of the house (De Angelis et al., 2013). As an example, let us consider a house having the length $\xi_1^{HS} = 20\,\text{m}$, $\xi_2^{HS} = 20\,\text{m}$, the height $\xi_3^{HS} = 4\,\text{m}$, a roof pitch of $\sigma^{HS} = 40^\circ$ and $\eta^{WI} = 6$ windows, each one with an area of $\Lambda^{WI} = 1\,\text{m}^2$. The thermal transmittance for walls and windows are assumed $\nu^{WA} = 0.15\,\text{W}\,\text{m}^{-2}\,\text{K}^{-1}$ and $\nu^{WI} = 1\,\text{W}\,\text{m}^{-2}\,\text{K}^{-1}$, respectively. The heat loss factor in this example house is calculated as follows:

$$\kappa^{HS} = \nu^{WA}\left(2\left(\xi_1^{HS}+\xi_2^{HS}\right)\xi_3^{HS} - \eta^{WI}\Lambda^{WI}\right) + \eta^{WI}\nu^{WI}\Lambda^{WI} = 191.16\,\text{kJ}\,\text{h}^{-1}\,^\circ\text{C} \tag{14}$$

By using the density of the air $\rho^{AR} = 1.2041\,\text{kg}\,\text{m}^{-3}$ at standard conditions, the total air mass is:

$$\mu^{HS} = \rho^{AR}\left(\xi_1^{HS}\xi_2^{HS}\xi_3^{HS} + 0.25\,\xi_1^{HS}\left(\xi_2^{HS}\right)^2\tan(\sigma^{HS})\right) = 3946\,\text{kg}. \tag{15}$$

For all the 60 residential houses, the indoor air masses and heat loss factors are presented in Figure

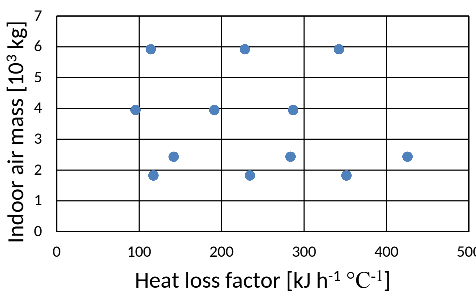


Figure 6: Indoor air masses and heat loss factors of the residential houses.

6. The set of houses used in the simulation has been obtained using all the possible combinations between the 5 thermal comfort profiles (Fig. 5) and the 12 different house characteristics (Fig. 6).

During the presentation of the test results, the benefits provided by the proposed DSM model are analyzed by comparing the results of the described optimization algorithm to those of two different simulations. In the first case, the term of comparison is given by a simulation where the target of the internal control system of the heat pump is to keep the indoor temperature as close as possible to the reference temperature $\Gamma^{RF}_{h,t}$ for all the time periods. This simulation has been run separately for each HP $h$ by using a QP approach that minimizes the squared difference of the indoor temperature of the house with respect to the reference temperature selected by the customer, according to:

$$\begin{aligned} \underset{y_{h,t},\Delta F^{HP}_{h,m,t}}{\text{minimize}} \quad & \sum_{t} \left(T^{IN}_{h,t} - \Gamma^{RF}_{h,t}\right)^2 \quad \forall h \\ \text{s.t.} \quad & \text{Eqs. } (1)-(11) \end{aligned} \tag{16}$$

This comparison aims at highlighting the advantages offered by the proposed DSM scheme with respect to a scenario in which no DSM is applied. In the following, this operation mode of the HP will be referred to as “internal HP control”.

In the second case, the DSM model has been approximated by using the same model presented in Section 3 but excluding multiple HP modes $m$. Thus, HP operation is only valid in mode $m = \{\text{m0}\}$ (by using the equality constraint Equation (7)) and Equation (8) is not required any more in the optimization. In this comparison, the binary operation of the heat pump is selected to have an air mass flow of $\Delta Phi^{UB}_{\text{m0}} = 647\,\text{kg}\,\text{h}^{-1}$ and a power per air mass flow $\beta_{\text{m0}} = 1.25\,\text{W}\,\text{h}\,\text{kg}^{-1}$. This value is the mean air mass flow of the continuous heat pump model. This scenario allows showing the different results achievable when considering a more realistic (continuous) operation mode of the heat pump rather than a simplified binary version.

## 4.2 Simulation Results

To assess the benefits provided by the proposed DSM scheme, a first simulation scenario, using as input the outdoor temperature of a day in May (see Fig. 5), has been considered. In this test case, it is assumed that the optimization has to be performed in a portion of a LV grid where all the 60 houses are equipped with an electric heat pump. In addition, an industrial load is also taken into account, which operates at $\{1.5\,\text{kW}, 8\,\text{kW}\}$ and switches with a period of 4 h, starting with 8 kW at midnight. This scenario can be representative, for example, of a distribution feeder that supplies the simulated 60 houses.

At the household level, the results for an example house are presented in Figure 7. The comparison of the scheduled powers of the heat pump, for the case of internal HP control and for the DSM with binary and continuous HP operation mode, is presented in the upper part of the figure, while the respective indoor temperatures are presented in the bottom part. In the case of temperature minimization in the internal control system of the heat pump, obviously the indoor temperature follows closely the reference temperature. It can be observed that more power is required in the morning, when the desired reference temperature increases, and that the heat pump works regardless of the loading conditions of the grid. With the DSM, since the optimization algorithm fosters the power consumption in some time periods more than in others, the full range of the specified temperature bounds is used. However, it is possible to observe that the temperature always falls within the range accepted by the customer. In particular, morning hours (when the loading of the grid is lower) are used to store thermal energy in the house, while during peak hours the operation of the heat pump is minimized in order not to aggravate the situation in the grid (while providing to the customer the required comfort).

The main differences between the binary and the proposed continuous HP operation mode are from an energy consumption perspective. Indeed, it is possible to see that the continuous model leads to operate the heat pump at lower power levels and for a longer time during the day. This allows better modulating the power before peak hours, when the storage of thermal energy is needed, and during peak hours, when, while respecting the customer thermal requirements, the operation of the heat pump has to be minimized. In addition, operating the HP at its lower bound also

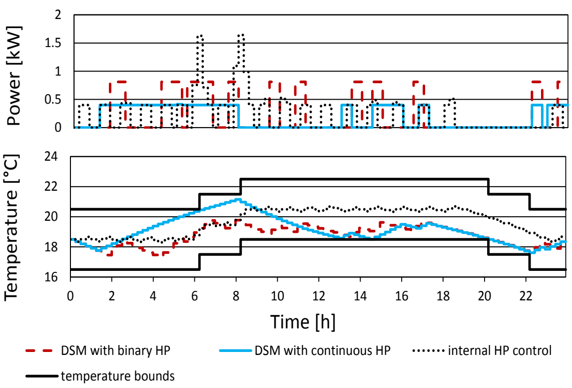


Figure 7: Heat pump consumptions and temperature profiles for one example house in the first simulation scenario.

Table 2: Results on the daily energy consumption, first simulation scenario.

| case | HP consumption (kWh) | increase (%) |
|---|---|---|
| *Example household* | | |
| DSM - continuous HP | 4.19 | - |
| DSM - binary HP | 5.88 | + 40.2 |
| internal HP control | 5.46 | + 30.2 |
| *Overall scenario* | | |
| DSM - continuous HP | 333.6 | - |
| DSM - binary HP | 459.4 | + 37.7 |
| internal HP control | 439.8 | + 31.8 |

allows using the most efficient operation points of the HP, and this implies a significant reduction in the overall energy consumption for the end-user. Table 2 shows the results related to the energy consumption for both the example household presented in Fig. 7 and for the overall scenario. It is possible to see that a simplified binary model of the HP clearly leads to a larger energy consumption, which may be not acceptable for the final customers.

The results obtained at the grid level are shown in Figure 8. Whereas for all the cases the inflexible industrial and residential loads are the same, the flexible parts differ depending on the HP scheduling. In this scenario, all the houses are equipped with heat pumps, so a large amount of flexible energy is available. As a consequence, the final curve of aggregated power is mainly determined by the allocation of this flexible energy, rather than by the shape of the fixed load. In the case of temperature minimization using the internal control of the HP, large power peaks are obtained. The reason for these peaks is the presence of similar comfort profiles for many customers (see Fig. 5), which leads to the simultaneous operation of the heat pumps. Even though these peaks are originated by the particular thermal requirements used for the test, this kind of problem is likely in a scenario with large penetration of electric HPs managed in a decentralized way. In fact, end-users can have same requirements

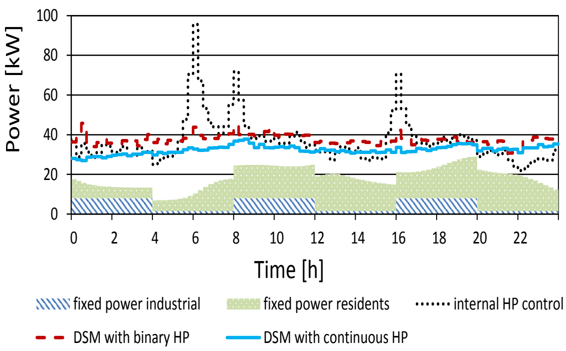


Figure 8: Aggregated power in the grid for the first simulation scenario.

Table 3: Technical benefits with the DSM at peak times, first simulation scenario.

| case | max. peak (kW) | power at 6:00 (kW) | HP cut (%) |
|---|---|---|---|
| internal HP control | 95.6 | 95.6 | - |
| DSM - binary HP | 45.8 | 43.8 | 60.9 |
| DSM - continuous HP | 37.8 | 32.7 | 73.9 |

in some periods of the day (e.g. due to similar working hours or consequently to the weather conditions) or price-based DSM programs can lead to a similar reaction of the customers. This would bring the simultaneous operation of the heat pumps, thus determining a significant impact on the aggregated power demand. The use of a centralized optimization approach leads significant benefits in this perspective, allowing to achieve power peak shaving. Fig. 8 clearly shows that a much flatter demand profile is obtained thanks to the application of the DSM. Table 3 reports the numeric results for the maximum power peaks originated by each HP control. It is possible to see that a reduction of the power peak larger than 60% is obtained for the DSM with continuous HP operation mode. Since the actual potential of the DSM scheme is only to manage the HP power, Table 3 also shows the results in terms of flexible energy that is shifted through the DSM to avoid the power peaks. Considering the power peak time for the case of internal HP control, almost 74% of the flexible power can be reallocated through the DSM scheme (this reduction is calculated considering only the part of the load associated to the HP operation). The continuous HP operation mode provides larger improvements due to its flexibility in choosing the HP operation point and its better efficiency with respect to the binary HP.

To evaluate the potential of the proposed DSM scheme even when less flexible energy is available, a second test case has been run considering a scenario with 240 residential houses, among which only 60 are endowed with electric HPs. This test case could be representative, for example, of a MV/LV substation that subtends four different feeders. Due to the assumed scenario, also the industrial load has been scaled up to consider four feeders, and power levels equal to $\{6\,\mathrm{kW}, 32\,\mathrm{kW}\}$ have been assumed using the same operation cycles as the previous test. While the same considerations as the previous case hold when looking at the single household, different results can be found when considering the aggregated power at grid level. Fig. 9 shows the obtained power profiles for the different HP operation modes. In this case, the level of the fixed load is relevant with respect to the flexible power associated to the HPs, thus the profile of the aggregated power is strongly affected by its shape. Nonetheless, it is possible to observe that,

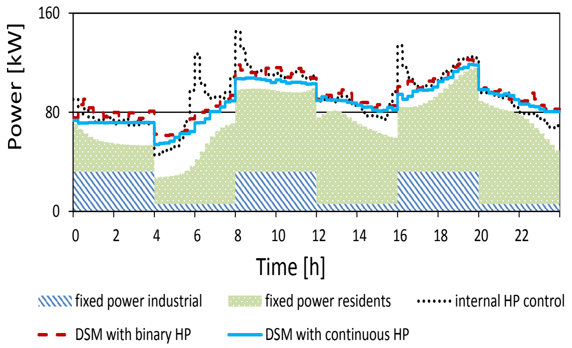


Figure 9: Aggregated power in the grid for the second simulation scenario.

when no DSM is applied, the three additional power peaks brought by the customer thermal requirements are still evident and give the largest power peaks over the day. In case of DSM, a power profile as flat as the one obtained in the previous test scenario cannot be found due to the relatively low amount of flexible energy. However, it is possible to note that the DSM scheme accomplishes its task of power peak minimization by reducing the HP use at the peak hours and scheduling the operation of the HPs during off-peak periods. This behaviour is clearly depicted in Figure 10, which shows the distribution of the HPs operation over the day for the two DSM schemes. It is possible to observe that, in the case of continuous HPs, all the devices are activated in the period of lowest power consumption (4:00 - 6:00), while only a minimum set of HPs is scheduled to operate during peak hours, like at 12:00 or at 20:00. Fig. 10 also permits underlining once more the advantages of the continuous HP mode with respect to the binary model. In the latter case, in fact, despite a generally lower use of the HPs (because they generally operate at higher power), the same or a larger number of HPs is running during peak periods, which implies a larger additional power due to the fixed power chosen to represent the binary behaviour. This is also reflected in Table 4, which shows the obtained values of power peak,

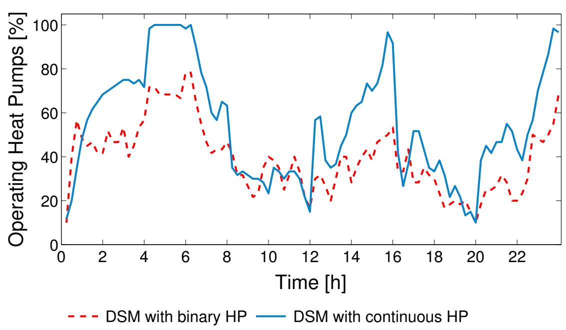


Figure 10: Distribution of the HP operation for the second simulation scenario.

Table 4: Technical benefits with the DSM at peak times, second simulation scenario.

| case | max. peak (kW) | HP power (kW) | operating HPs |
|---|---|---|---|
| internal HP control | 145.1 | 47.2 | 40 |
| DSM - binary HP | 122.7 | 9.7 | 12 |
| DSM - continuous HP | 118.6 | 3.2 | 9 |

the corresponding quote brought by the HPs, and the number of HPs operating at that time. Moreover, even in this scenario, the binary HP model proves to be less efficient than the continuous one, with an increase in the overall energy consumption (for all the 60 houses) larger than 36%.

To further confirm the results achieved until now, the last scenario has been simulated again considering as outdoor temperature a day in December (see Fig. 5). The first consideration in this test case concerns the DSM with binary HPs: in these conditions the optimization algorithm is unable to find a feasible solution, because with the considered operating power is not possible to fulfil the thermal comfort requirements during the changes in the reference temperature. This outcome highlights once again the possible drawbacks associated to the introduction of this simplification in the HP model. Focusing on the other two HP scheduling criteria, Figure 11 shows the results obtained for the aggregated power at grid level. Comparing these results with those obtained in the same scenario in May (Fig. 9), it is immediate to verify that a larger amount of HP energy results on top of the inflexible base load. This is a consequence of the colder outdoor temperature, which forces the HPs to run more frequently in order to provide the required thermal comfort to the customers. Looking at the scheduling of the single households, in the case of DSM with continuous HP, 5 houses out of 60 require to have the HP running at all the time steps, and 13 houses need an operating HP for at least 23 hours. These effects are automatically propagated to the results of the ag-

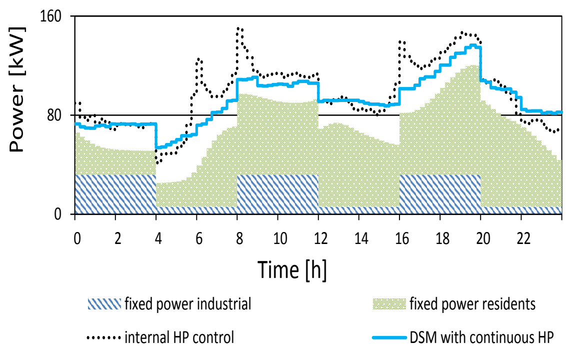


Figure 11: Aggregated power in the grid for the third simulation scenario.

Table 5: Technical benefits with the DSM at peak times, third simulation scenario.

| case | max. peak (kW) | HP power (kW) | operating HPs |
|---|---|---|---|
| internal HP control | 149.8 | 52.5 | 43 |
| DSM - continuous HP | 136.5 | 14.9 | 28 |

gregated power. As shown in Table 5, in fact, the level of power and the number of operating HPs during the peak time is significantly larger than in the previous simulation scenario. Nonetheless, despite this slight degradation of the DSM performance, it is still possible to notice as the proposed DSM scheme allows optimizing the scheduling of the HPs, reducing as much as possible the operation at the peak time and filling the valleys during off-peak hours. In comparison to the case of internal HP control, a reduction of the power peak and of the overall energy consumption larger than 9% and 20%, respectively, is obtained also in this last scenario.

Finally, as for the computational cost for the proposed method, we can state that it is relatively low. The test cases were solved on a standard laptop using CPLEX 12.7.0.0 in GAMS 24.8 on an Intel i7(2.9 GHz) machine with 16 GB RAM. The termination criteria for the DSM with binary and continuous operation mode was set to a computation time of 2400 s and 1200 s, respectively; thus, both optimizations were not solved to global optimality. This is reasonable since sub-optimal solutions from the grid perspective are achieved quickly. Table 6 shows the results related to the first presented simulation scenario. Note, before the relative gap is calculated all separate parameters and products of multiple parameters that arise in the objective function are subtracted from the objective function. Interestingly, the more detailed the HP model, the smaller gets the relative gap. This means that a more realistic model (continuous HP operation) decreases the computational complexity of the problem. As for the internal HP control case, where the temperature differences are minimized, a QP optimization is solved for each house (in total 60). The termination criteria of each optimization was set to a computation time of 300 s. The relative gap of the 60 QPs varies much, but the majority was solved to global optimality.

Table 6: Computational results.

| case | time (s) | relative gap (%) |
|---|---|---|
| internal HP control | 10922 | differs |
| DSM with binary HP | 2400 | 8.15 |
| DSM with continuous HP | 1200 | 1.33 |

# 5 CONCLUSIONS

This paper presented an optimization algorithm designed to define the day ahead scheduling of heat pumps for achieving power peak shaving in the electric grid. The conceived approach exploits the flexibility given by the heating devices on the customer side to obtain the minimization of the power peaks, while providing the required thermal comfort to the final users. Performed tests prove that the proposed approach allows combining the benefits for the utilities with the service for the customer, which obtains the required temperature over the day and a minimization of the energy consumption. Moreover, the advantages brought by the proposed continuous operation model of the heat pump, with respect to the simplified case of binary operation of the heat pump, are presented. This work will be used as a starting point for further developments in this field. In particular, a deeper study on the impact of the customer flexibility on the final results and the evaluation of the possible drawbacks led by the unavoidable uncertainties present in the used model (e.g. outdoor temperature, knowledge of the building parameters, etc.) will be object of future studies. The possible use of dedicated thermal storage will be also object of future work, since it can significantly increase the available flexibility leading to potential improvements in the achievable results and in the design of the DSM scheme. The integration of additional home appliances in the proposed management algorithm can be a further step for the design of a complete DSM program fully exploiting the flexibility offered by residential customers.

# ACKNOWLEDGEMENTS

This work was supported by FLEXMETER, which is an EU Horizon 2020 project under grant agreement no. 646568.

# REFERENCES

Akmal, M. and Fox, B. (2016). Modelling and simulation of underfloor heating system supplied from heat pump. In *2016 UKSim-AMSS 18th International Conference on Computer Modelling and Simulation (UKSim)*, pages 246–251.

Arteconi, A., Hewitt, N., and Polonara, F. (2013). Domestic demand-side management (dsm): Role of heat pumps and thermal energy storage (tes) systems. *Applied Thermal Engineering*, 51(1):155–165.

Balijepalli, V. S. K. M., Pradhan, V., Khaparde, S. A., and Shereef, R. M. (2011). Review of demand response under smart grid paradigm. In *ISGT 2011 India*, pages 236–243.

Bhattarai, B. P., Bak-Jensen, B., Pillai, J. R., and Maier, M. (2014). Demand flexibility from residential heat pump. In *2014 IEEE PES General Meeting — Conference Exposition*, pages 1–5.

Caprino, D., Vedova, M. L. D., and Facchinetti, T. (2014). Peak shaving through real-time scheduling of household appliances. *Energy and Buildings*, 75:133 – 148.

Chapman, N., Zhang, L., Good, N., and Mancarella, P. (2016). Exploring flexibility of aggregated residential electric heat pumps. In *2016 IEEE International Energy Conference (ENERGYCON)*, pages 1–6.

Csetvei, Z., Østergaard, J., and Nyeng, P. (2011). Controlling price-responsive heat pumps for overload elimination in distribution systems. In *2011 2nd IEEE PES International Conference and Exhibition on Innovative Smart Grid Technologies*, pages 1–8.

De Angelis, F., Boaro, M., Fuselli, D., Squartini, S., Piazza, F., and Wei, Q. (2013). Optimal home energy management under dynamic electrical and thermal constraints. *Industrial Informatics, IEEE Transactions on*, 9(3):1518–1527.

Fan, J. and Borlase, S. (2009). The evolution of distribution. *IEEE Power and Energy Magazine*, 7(2):63–68.

FERC (2011). Assessment of demand response and advanced metering. *Federal Energy Regulatory Commission, Washington DC, USA, Staff Report*.

Good, N., Zhang, L., Navarro-Espinosa, A., and Mancarella, P. (2013). Physical modeling of electro-thermal domestic heating systems with quantification of economic and environmental costs. In *Eurocon 2013*, pages 1164–1171.

Hedman, K. W., O'Neill, R. P., and Oren, S. S. (2009). Analyzing valid inequalities of the generation unit commitment problem. In *Power Systems Conference and Exposition, 2009. PSCE'09. IEEE/PES*, pages 1–6. IEEE.

Klaassen, E., Kobus, C., Frunt, J., and Slootweg, H. (2016a). Load shifting potential of the washing machine and tumble dryer. In *2016 IEEE International Energy Conference (ENERGYCON)*, pages 1–6.

Klaassen, E. A. M., Frunt, J., and Slootweg, J. G. (2016b). Experimental validation of the demand response potential of residential heating systems. In *2016 Power Systems Computation Conference (PSCC)*, pages 1–7.

Kouzelis, K., Tan, Z. H., Bak-Jensen, B., Pillai, J. R., and Ritchie, E. (2015). Estimation of residential heat pump consumption for flexibility market applications. *IEEE Transactions on Smart Grid*, 6(4):1852–1864.

Li, W. T., Gubba, S. R., Tushar, W., Yuen, C., Hassan, N. U., Poor, H. V., Wood, K. L., and Wen, C. K. (2017). Data driven electricity management for residential air conditioning systems: An experimental approach. *IEEE Transactions on Emerging Topics in Computing*, PP(99):1–1.

Loesch, M., Hufnagel, D., Steuer, S., Faßnacht, T., and Schmeck, H. (2014). Demand side management in smart buildings by intelligent scheduling of heat pumps. In *2014 IEEE International Conference on Intelligent Energy and Power Systems (IEPS)*, pages 1–6.

Molitor, C., Ponci, F., Monti, A., Cali, D., and Müller, D. (2011). Consumer benefits of electricity-price-driven heat pump operation in future smart grids. In *2011 IEEE International Conference on Smart Measurements of Future Grids (SMFG) Proceedings*, pages 75–78.

Nielsen, K. M., Pedersen, T. S., and Andersen, P. (2012). Heat pumps in private residences used for grid balancing by demand desponse methods. In *PES T D 2012*, pages 1–6.

SEDC (2014). Mapping demand response in europe today. *Smart Energy Demand Coalition, Brussels, Belgium, Technical Report*.

Strbac, G. (2008). Demand side management: Benefits and challenges. *Energy Policy*, 36(12):4419–4426.

US DoE (2006). Benefits of demand response in electricity markets and recommendations for achieving them. *US Dept. Energy, Washington DC, USA, Technical Report*.